Tetrahedrally bonded dense C_2N_3H with a defective wurtzite structure: X-ray diffraction and Raman scattering results at high pressure and ambient conditions

Ashkan Salamat, Katherine Woodhead, Paul F. McMillan,* Raul Quesada Cabrera, Aisha Rahman, Davy Adriaens, and Furio Corà
Department of Chemistry and Materials Chemistry Centre, University College London, 20 Gordon Street, London WC1H 0AJ, United Kingdom

Jean-Philippe Perrillat
European Synchrotron Radiation Facility, BP 220, 38043 Grenoble Cedex, France
(Received 18 May 2009; revised manuscript received 13 August 2009; published 17 September 2009)

Synchrotron x-ray diffraction and Raman scattering data supported by *ab initio* calculations are reported for the dense tetrahedrally bonded phase (C_2N_3H) with a defective wurtzite (dwur) structure synthesized by laser heating from dicyandiamide ($C_2N_4H_4$) at high pressure in a diamond anvil cell. This work confirms the structure deduced in previous work from electron diffraction experiments. The phase ($Cmc2_1$) is recoverable to ambient conditions. The ambient pressure volume (V_0=137.9 Å^3) and bulk modulus (K_0=258±21 GPa) are in excellent agreement with density functional calculations (V_0=134.7 Å^3; K_0=270 GPa). The calculated Raman frequencies and pressure shifts are also in good agreement with experiment. Ammonia ($P2_12_12_1$) was identified among the reaction products as expected from the synthesis reaction.

DOI: 10.1103/PhysRevB.80.104106 PACS number(s): 62.50.−p, 31.15.A−, 61.50.Ks

I. INTRODUCTION

Since the theoretical prediction that sp^3-bonded forms of carbon nitride (C_3N_4) might be superhard[1,2] there has been intense interest in developing high-density materials within the C-N-H system. Such compounds could also have applications for energy storage.[3] Analogous compounds include refractory ceramics based on Si_3N_4 (Ref. 4) and Ga, Ge containing nitrides that provide wide band-gap materials for optoelectronics applications.[5] High-pressure, high-temperature (HPHT) synthesis experiments have resulted in spinel-structured forms of Si_3N_4 (Ref. 6) and Ga_3O_3N (Refs. 7 and 8) with low compressibility, high hardness, and wide band gaps. These materials were prepared by direct synthesis from the elements or using molecular precursors treated under HPHT conditions. Various dense C_xN_y and $C_xN_yH_z$ materials have been produced using physical or chemical vapor deposition methods but their structure, properties, and chemical composition have not yet been fully determined.[9–11]

Horvath-Bordon *et al.*[12] recently reported the synthesis of a new solid state compound C_2N_3H prepared from the molecular precursor dicyandiamide (DCDA: C_2N_3H) in a laser-heated diamond anvil cell (LH-DAC) at P>27 GPa and T ~1800 K. The new material was recovered to ambient conditions. Several grains were studied by electron energy loss spectroscopy in the TEM along with nano-SIMS to determine the chemical composition and show that C and N were tetrahedrally bonded with sp^3 hybridization.[13] The structure was studied using electron diffraction. The results combined with density functional theory (DFT) predictions indicated the structure was of a defective wurtzite (dwur) type as found in Si_2N_2O, $Si_2N_2(NH)$ (i.e., Si_2N_3H). The structure of dwur C_2N_3H is related to a tripled 3×3 cell of hexagonal C-lonsdaleite. N atoms occupy one set of tetrahedral sites and tetrahedral C atoms fill 2/3 of the other sublattice. The remaining positions are filled with H atoms bound to N (Fig. 1). In the present work, we have obtained x-ray diffraction (XRD) data in the DAC at high pressure and during decompression that confirms the structural model and that no phase transitions occur upon release of pressure and recovery to ambient conditions. The results are also confirmed by Raman spectra obtained following synthesis in the DAC and during decompression.

II. EXPERIMENTAL TECHNIQUES

Dicyandiamide ($C_2N_4H_4$: Aldrich, 99%) was loaded under O_2/H_2O-free conditions into cylindrical DACs using either sodium chloride (NaCl) or lithium fluoride (LiF) as a pressure-transmitting medium (PTM) and to provide thermal insulation to the diamond windows during laser heating experiments. We found no evidence for reactions occurring between the C-N-H phases and the PTM during synthesis experiments. The choice of PTM was an important issue for the x-ray diffraction experiments. NaCl has been well tested for LH-DAC experiments but it has strong diffraction lines that mask some of the key reflections of the C_2N_3H phase. The situation is further complicated by the B1-B2 transition that occurs at P ~27 GPa and with considerable hysteresis during decompression.[14] LiF is less well established as a PTM for LH-DAC synthesis studies: however, we found it per-

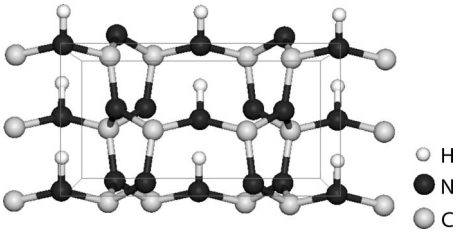

FIG. 1. C_2N_3H with a defective wurtzite (dwur) structure.

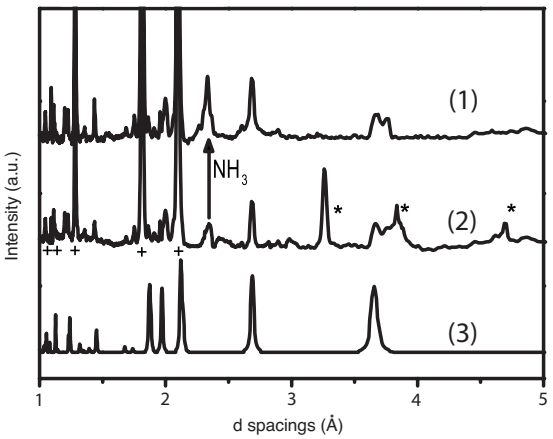

FIG. 2. XRD patterns obtained at 45 GPa following LH-DAC synthesis of dwur-C_2N_3H from DCDA. (1) Pattern obtained after extended heating and pattern (2) is captured beforehand during the initial heating period. Additional peaks (*) correspond to an unidentified C-N-H metastable phase formed during the initial synthesis reaction. The main peak of NH_3-III is identified in both experimental patterns. (3) Corresponding calculated pattern (DFT) at 45 GPa. [(+) indicate Bragg peaks from LiF, used as PTM].

formed well during these experiments and its use enabled us to complete the set of diffraction data observed for C_2N_3H.

Rhenium gaskets were preindented to 30 μm with 100 μm holes drilled by electro-erosion and used to contain the samples. Pressures were determined by ruby fluorescence.[15] The pressure was raised initially to 30–45 GPa and samples were heated to $T \sim 2500-2800$ K using either a 150 W CO_2 laser (10.6 μm) at UCL or a Nd^{3+}:YAG laser (1.064 nm) at ESRF. Tests using Nd^{3+}:YAG laser heating were also conducted at UCL prior to the synchrotron runs. For Nd^{3+}:YAG LH-DAC experiments Re powder was mixed with the sample (100:1 ratio) to couple with the near-IR laser beam. XRD experiments were carried out at beamline I15 of Diamond Light Source (Didcot, UK: $\lambda_0 = 0.350714$ Å) and at ID27 of the European Synchrotron Radiation Facility (Grenoble, France: $\lambda_0 = 0.26473$ Å). Some preliminary studies were also carried out at station 9.5 of the Synchrotron Radiation Source (Daresbury, UK: $\lambda_0 = 0.443970$ Å).[16] Diffraction patterns were recorded as two-dimensional (2D) angle-dispersive data sets using MAR image plate or charged couple device (CCD) detectors: the data were transformed to intensity vs wavelength/energy/d-value spectra and analyzed using FIT2D[17] and FULLPROF[18] software packages. Raman spectra were obtained at University College London with 514.5 nm Ar^+ laser excitation using a home-built high-throughput optical system based on Kaiser supernotch filters, an Acton spectrograph and LN_2 cooled back-thinned CCD detector or using an inVia Renishaw micro-Raman system using 785 nm excitation.

DFT calculations were carried out under periodic boundary conditions using CRYSTAL06.[19] We employed two different hybrid-exchange functionals, namely, B3LYP[20] and PBE0.[21] All atoms were described with an all electron 6–21G** basis set,[22] apart from the ambient pressure Raman mode calculation, which used Pople 6–21G* basis sets for C and N atoms and 8111G* for H atoms. Full geometry optimizations of the periodic systems were carried out to determine local minima on the potential energy surface (PES) using analytical gradients of the energy with respect to atomic positions and cell parameters. Symmetry was preserved throughout the optimizations. The SCF convergence threshold was set to 1×10^{-7} Hartree on the total energy. Calculations were performed using Pack-Monckhorst grids for integration in reciprocal space, with k-point nets of $4 \times 4 \times 4$. Geometry optimization was checked against root mean square (RMS) and absolute value of the largest component for both gradients and nuclear displacements, and considered complete when four conditions are simultaneously satisfied for both fractional coordinates and unit cell parameters, using the default values of 4.5×10^{-4} for the maximum gradient and 1.8×10^{-3} for the maximum displacement (all measured in a.u). Zone center phonons were calculated at the optimized structure for each pressure, using numerical differentiation of the analytical gradients of the energy with respect to atomic displacements using Cartesian displacements of 0.001 Å and a tighter convergence tolerance of 1×10^{-9} Ha in the total energy. The effects of pressure were simulated by performing a series of constant volume geometry optimizations for all structures, in which the volume varied between 109% and 80% of the ambient-pressure value. Following the constant-volume optimizations, a cubic fit to the internal energy (E) vs volume (V) curve was used to obtain pressure and enthalpy. Bulk moduli and their first derivatives were obtained from the E(V) results using a third-order Birch-Murnaghan equation of state. Simulated XRD patterns were created using PowderCell.[23]

TABLE I. Lattice parameters and refined fractional coordinates of dwur-C_2N_3H ($Cmc2_1$) at ambient conditions.

Lattice parameters	a (Å)	b (Å)	c (Å)
	7.618 (5)	4.483 (2)	4.038 (1)
Fractional coordinates	x	y	z
C	0.325 (3)	0.328 (3)	0
N1	0.310 (1)	0.364 (4)	0.358 (2)
N2	0	0.285 (3)	0.422 (4)

III. RESULTS AND DISCUSSION

A. X-ray Diffraction

We obtained x-ray diffraction patterns (Diamond) for samples synthesized from the DCDA precursor in the DAC at pressures ranging from 30–45 GPa following laser heating at UCL and also *in situ* during laser heating experiments combined with synchrotron XRD at the ESRF. Our preliminary studies indicated that several C-N-H phases might coexist metastably within the sample following initial heating and that either prolonged heating (~15 mins) or several consecutive laser heating runs were necessary to fully convert the material to a single phase (Fig. 2). Those preliminary findings are confirmed in this study and the results are discussed below. Following prolonged heating in the DAC, an x-ray diffraction pattern was obtained that could be fully

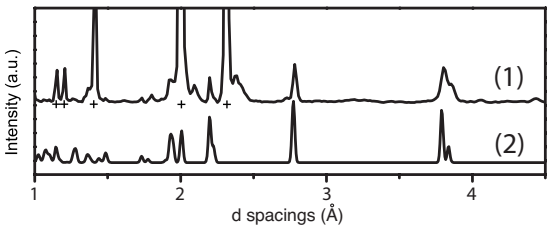

FIG. 3. XRD patterns for the dwur-C_2N_3H structure at ambient conditions: (4) Pattern of recovered sample after LH-DAC synthesis. (5) Predicted pattern from DFT calculations. [(+) indicates Bragg peaks from LiF, used as PTM].

assigned to dwur C_2N_3H, in agreement with the structure suggested previously from electron diffraction and DFT calculations.[12] Identification of nearly the full set of predicted diffraction peaks for each pressure recorded was made possible by combining data from several runs carried out using both NaCl and LiF PTM in the DAC during decompression. The lattice parameters of the structure recovered to ambient conditions were determined by LeBail refinement: a=7.618 Å, b=4.483 Å, c=4.038 Å (V_0=137.904 Å^3) within space group $Cmc2_1$ (Table I), in excellent agreement with DFT predictions (Fig. 3 and Table IV). Rietveld refinement was carried out on the ambient pressure sample following recovery, allowing the fractional coordinates of the atomic positions to be determined (Table I).

Following LH-DAC synthesis at 45 GPa x-ray diffraction patterns were recorded during decompression to ambient conditions. Approximately 20 of the predicted reflections could be followed throughout the decompression process when examining data from experiments using the 2 different PTMs. Table II shows the ten most intense peaks at ambient conditions that are possible to follow throughout decompression using LiF as the PTM. That result confirms that the dwur-C_2N_3H phase produced by laser heating in the DAC from the DCDA precursor is fully recoverable to ambient conditions, that no decomposition or phase transitions occur during decompression, and thus that it has the chemical composition and structure deduced from electron diffraction,

TABLE II. The crystal structure of dwur C_2N_3H at ambient conditions. The ten most intense reflections, that are possible to follow throughout decompression, are noted.

hkl	d (calc) (Å)	I (calc) (%)	d (exp) (Å)	I (exp) (%)
110	3.832	25	3.869	49
200	3.786	81	3.808	91
111	2.768	100	2.780	100
020	2.221	27	2.246	28
310	2.195	78	2.210	65
002	2.002	57	2.008	48
021	1.942	34	1.960	54
311	1.925	44	1.936	59
211	1.712	16	1.724	15
330	1.277	24	1.290	18

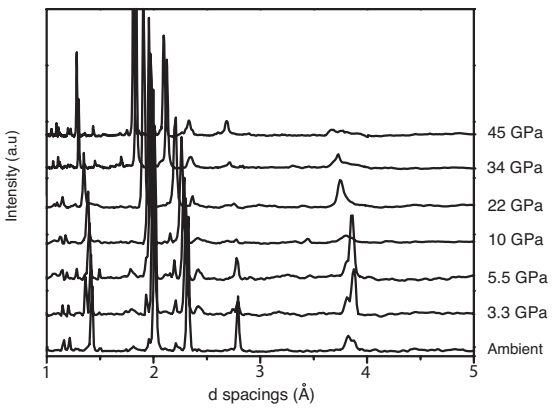

FIG. 4. XRD pattern obtained during decompression following LH synthesis of DCDA in the DAC at pressure to ambient P, T conditions using LiF PTM

EELS and nano-SIMS experiments on recovered materials combined with DFT predictions.[12] This then constitutes a high-density tetrahedrally bonded material produced in the C-N-H system that might have interesting and useful properties in its own right, as well as providing a potential precursor to dense carbon nitride phases.

We used the synchrotron x-ray diffraction data to construct a P(V) plot and evaluate the molar volume and compressibility parameters of the dwur-C_2N_3H phase (Figs. 4 and 5). The data were analyzed using a finite strain Birch-Murnaghan equation of state (EOS) expression expanded to third order:[24]

$$P(V) = 3K_0 f(1+2f)^{5/2}\left[1+\frac{3}{2}(K_0'-4)f\right] \quad (1)$$

Here K_0 is the zero pressure bulk modulus and K_0' its pressure derivative. Transforming the volume strain into the reduced variable

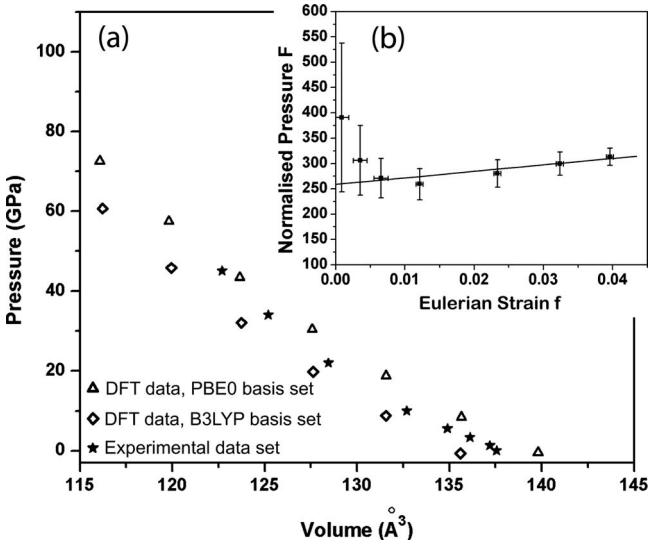

FIG. 5. (a) P(V) plot of structure A from DFT, PBEO (K_0 =288 GPa), and B3LYP (K_0=270 GPa) against the experimental data (K_0=258 GPa) (b) Normalized pressure (F) vs Eulerian strain (f)

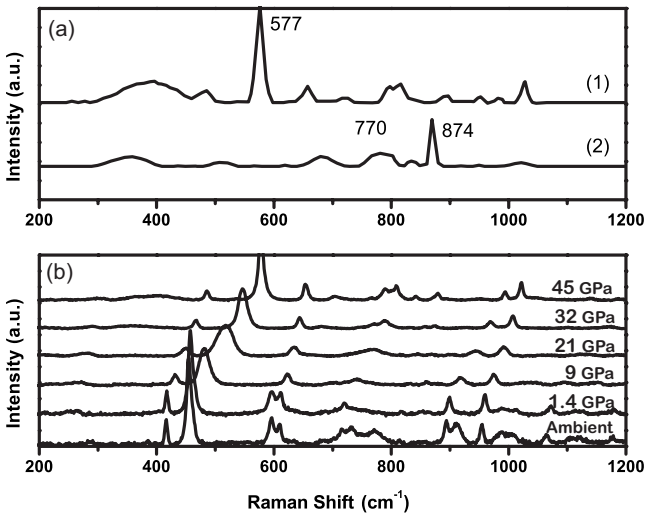

FIG. 6. (a) Raman spectra obtained following initial and extended laser heating of DCDA in a DAC at 45 GPa. (1) Spectrum of the dwur-C_2N_3H structure after extended LH. (2) Spectrum of an intermediate metastable phase formed during the initial stages of the heating reaction. (b) Raman spectra obtained following the decompression of dwur C_2N_3H from 45 GPa to ambient conditions.

$$f = \frac{1}{2}\left[\left(\frac{V_0}{V}\right)^{2/3} - 1\right] \tag{2}$$

and using a normalized pressure F defined by:

$$F = P[3f(1+2f)^{5/2}]^{-1} \tag{3}$$

provides a linearized version of the P(V) equation for useful determination of K_0 and K_0' values[21] [Fig. 5(b)]. The data indicate a bulk modulus value $K_0 = 258 \pm 21$ GPa with $K_0' = 6.3 \pm 0.8$ in good agreement with theoretical calculations ($K_0 = 271$ GPa, $K_0' = 3.97$: B3LYP; $K_0 = 288$ GPa, $K_0' = 3.94$: PBE0: Table IV). The bulk modulus for dwur C_2N_3H is comparable with that determined for the refractory high-hardness ceramic Si_3N_4 ($K_0 = 256$ GPa).[4]

B. Raman Spectroscopy

In our initial studies of synthesis of C_2N_3H from the DCDA precursor we reported a Raman spectrum taken in situ at high pressure in the DAC that contained sharp peaks at 577 and 874 cm^{-1} and a broader asymmetric band at 770 cm^{-1}. The 770 cm^{-1} band varied in relative intensity between syntheses carried out at MPI Mainz (Germany) and at UCL. During the present runs a doublet remains in this region but with greatly reduced intensity. We conclude that the strong broad 770 cm^{-1} feature observed in the initial runs is mainly due to a metastable C-N-H phase formed during the LH-DAC synthesis. In the present study, we have now determined that the 577 and 874 cm^{-1} peaks correspond to different phases. After initial laser heating in the DAC at 30–45 GPa a spectrum is obtained that is dominated by the 874 cm^{-1} peak and there is no evidence for the 577 cm^{-1} feature: after prolonged heating, the 874 cm^{-1} peak disappears and the 577 cm^{-1} band dominated the spectrum at high pressure [Fig. 6(a)]. That material is assigned from our in situ x-ray diffraction results to the dwur-C_2N_3H structure. During decompression this feature remained as the dominant peak in the 440–600 cm^{-1} region. It is assigned to the dwur-C_2N_3H from our DFT calculations (Table III).

TABLE III. Frequencies and symmetries of experimental and theoretical predicted active modes for C_2N_3H at ambient pressure. All the bands are Raman active although the A_2 are expected to be weak. In addition, with the exception of the A_2 bands the rest are also IR active. The corresponding experimentally determined Grüneisen parameters are also given.

(Calc) Peak position (cm^{-1})	(Exp) Peak position (cm^{-1})	Symmetry	(Exp) I (%)	(Exp) Grüneisen parameter
394	410	A_1	22	1.003
442	460	B_1	14	-
444	449	A_1	100	1.620
458		A_2		
583	592	B_1	13	-0.380
613	605	A_1	19	0.432
654		A_2		
663		B_2		
715	714	A_1	28	0.752
716	728	A_1	17	
769	773	B_1	46	0.509
780		A_2		
809		B_2		
850		A_2		
903	891	B_2	21	0.639
907	908	A_1	48	-
938	953	A_1	22	0.395
983	988	B_1	32	0.505
1033		A_2		
1034	1004	A_1	12	0.806
1056	1065	B_2	11	0.733
1067		B_2		
1070		A_2		
1099	1091	B_1	28	0.622
1104	1114	B_2	19	0.679
1120		A_2		
1124	1147	B_1	36	0.678
1180	1170	A_1	18	0.766

For the $Cmc2_1(C_{2v}^{12})$ structure we expect 33 Raman active vibrations:

$$\Gamma_{Raman} = 9A_1 + 8A_2 + 7B_1 + 9B_2 \tag{4}$$

We observe 16 peaks occurring between 200–1300 cm^{-1} that can be assigned to vibrational modes of dwur-C_2N_3H with symmetry species defined by the DFT calculations (Table III). All of the modes observed in the DAC at high pressure following the complete laser-heating synthesis could be followed to ambient conditions (Fig. 6(b)).

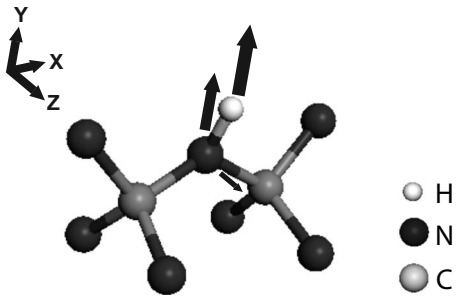

FIG. 7. The N and H displacements for the dominant A_1 Raman-active mode of dwur-C_2N_3H at 450–600 cm^{-1} are illustrated from DFT calculation results.

In addition the experimental mode Grüneisen parameters were defined by:

$$\gamma_i = \left(\frac{\partial \ln \omega}{\partial \ln V}\right)_{(T)} = \frac{K_0}{\omega_0}\left(\frac{\partial \omega}{\partial P}\right)_{(T)} \quad (5)$$

During decompression the dominant Raman peak at 440–600 cm^{-1} range exhibits significant broadening at ~21 GPa [Fig. 6(b)]. From examination of the calculated mode eigenvector we identify this as an A_1 symmetry mode due to a deformation vibration of the C-N-C linkage coupled with a large displacement of the H atoms (Fig. 7). That result indicates that some change might occur in the N-H ordering pattern within the dwur-C_2N_3H structure during decompression. That possibility is examined below using DFT calculations. We did not observe the N-H stretching modes predicted to occur at 3046 and 3131 cm^{-1}, and the N-H bending mode at 1594 cm^{-1} is only observed weakly in the high-pressure spectra.

C. Density Functional Theorem

In addition to providing support and interpretation for the x-ray diffraction and Raman spectroscopy results DFT calculations were used to investigate N-H bond rearrangements that might occur within the unit cell during decompression by considering different proton-ordered phases of the dwur-C_2N_3H structure. This part of the study was motivated by the observation that the dominant Raman peak in the 450–600 cm^{-1} region exhibited noticeable broadening during decompression at P ~ 21 GPa [Fig. 6(b)]. A full geometry optimization using both DFT methods was carried out for three C_2N_3H systems with different N-H ordering patterns within space groups $Cmc2_1$ or $Pmc2_1$) (Table IV). In Structure A the dwur unit cell has H atoms in identical sites with the N-H vectors aligned in the same direction. In Structure B, the H atoms occupy opposing axial positions, and Structure C contains a mixture of A and B structural units (Fig. 9). Energy optimizations within the three structures all converged and suggested that they might each occupy a subsidiary minimum within the potential energy surface. However, the energies are indistinguishable indicating that the structure formed experimentally might correspond to any one of the possibilities, or to an average among the structures with different N-H bonding patterns. The different structures examined by DFT methods have indistinguishable structural and compressibility parameters (Table IV).

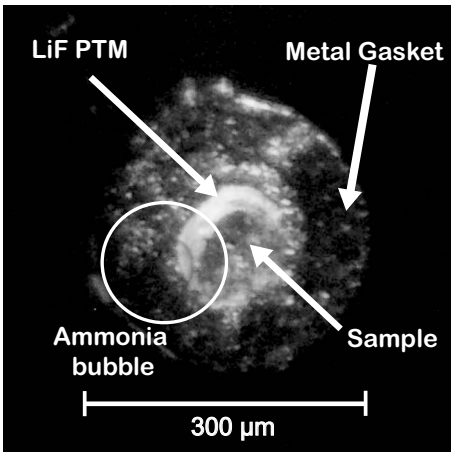

FIG. 8. A photograph looking through the top anvil of the DAC into the sample chamber upon opening. The ring shows a bubble of ammonia effervescing through the sample chamber. Available as a video sequence from the authors on request

TABLE IV. A comparison of ambient-P lattice parameters and bulk modulus values calculated (DFT) for different N-H ordered phases of dwur C_2N_3H and that of the experimental data.

	PBE0			B3LYP			
Structure	A	B	C	A	B	C	Experimental
Space Group	$Cmc2_1$	$Cmc2_1$	$Pmc2_1$	$Cmc2_1$	$Cmc2_1$	$Pmc2_1$	$Cmc2_1$
a (Å)	7.580	7.583	7.581	7.656	7.663	7.659	7.618
b (Å)	4.447	4.393	4.421	4.500	4.447	4.475	4.483
c (Å)	4.023	4.065	4.043	4.058	4.102	4.079	4.038
K_0 (GPa)	288	281	285	271	264	267	258 (21)
K_0'	3.94	4.18	4.04	3.97	4.01	3.94	6.3(0.8)
Vol ($Å^3$)	135.596	135.399	135.510	139.803	139.786	139.824	137.904(0.126)

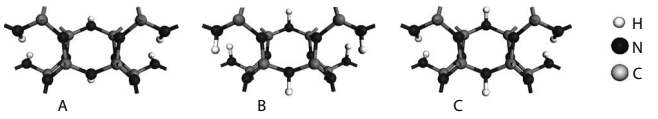

FIG. 9. The figure illustrates the three N-H phases investigated by DFT.

IV. DISCUSSION

Since the first report of synthesis of dwur-C_2N_3H from DCDA ($C_2N_4H_4$) by LH-DAC methods at $P > 27$ GPa and $T \sim 1800$ K it has been assumed that the reaction proceeds by elimination of NH_3 to produce the solid-state compound. That reaction has now been confirmed by our synchrotron x-ray results that show the appearance of solid NH_3 (phase III: $P2_12_12_1$)[25,26] identified in the diffraction patterns at high pressure and during decompression (Fig. 2). During the final stages of decompression the ammonia solid phase becomes liquid and escapes from the cell (Fig. 8). The principal broad peak of solid NH_3 at 2.3 Å could be followed during decompression down to 5 GPa.

V. CONCLUSION

Using a combination of synchrotron XRD and Raman spectroscopy supported with DFT calculations we conclude that the high-density dwur-structured compound C_2N_3H is produced by heating DCDA ($C_2N_4H_4$) as a molecular precursor at high pressure. This C_2N_3H phase is recoverable to ambient conditions and it has a large bulk modulus comparable with high hardness silicon nitride ceramics. An unidentified metastable C-N-H phase is also produced during the initial synthesis reaction. Recently Liu *et al.*[27] identified XRD lines that they assigned to the theoretically predicted phase β-C_3N_4 among the products of their shock synthesis experiments using DCDA as a precursor. Our results indicate that the XRD pattern obtained by Liu *et al.* likely corresponds mainly to dwur C_2N_3H along with some intermediate phases produced by high-P, T shock synthesis.

ACKNOWLEDGMENTS

This work was supported by EPSRC Portfolio Grant No. EP/D504782 and an EPSRC (Grant No. EP/D07357X) to PFM. During early experiments at the SRS we thank Alistair Lennie for his support and we thank Domink Daisenberger for discussion. We also acknowledge the assistance of Monica Amboage at Diamond Light for help with experiments at I15 and Mohamed Mezouar for access and help with facilities at ESRF.

*p.f.mcmillan@ucl.ac.uk

[1] A. Y. Liu and M. L. Cohen, Science **245**, 841 (1989).
[2] D. M. Teter and R. J. Hemley, Science **271**, 53 (1996).
[3] X. C. Wang, K. Maeda, A. Thomas, K. Takanabe, G. Xin, J. M. Carlsson, K. Domen, and M. Antonietti, Nature Mater. **8**, 76 (2009).
[4] R. Riedel, *Handbook of Ceramic Hard Materials* (Wiley, New York, 2008), Vol. 1.
[5] F. A. Ponce and D. P. Bour, Nature (London) **386**, 351 (1997).
[6] E. Soignard, M. Somayazulu, J. Dong, O. F. Sankey, and P. F. McMillan, J. Phys.: Condens Matter **13**, 557 (2001).
[7] I. Kinski, G. Miehe, G. Heymann, R. Theissmann, R. Riedel, and H. Huppertz, Z. Naturforsch., B: Chem. Sci **60**, 831 (2005).
[8] E. Soignard, D. Machon, P. F. McMillan, J. Dong, B. Xu, and K. Leinenweber, J. Mater. Chem. **17**, 5465 (2005).
[9] J. P. Riviere, D. Texier, J. Delafond, M. Jaouen, E. L. Mathe, and J. Chaumont, Mater. Lett. **61**, 2855 (2007).
[10] M. Lejeune, O. Durand-Drouhin, K. Zellama, and M. Benlahsen, Solid State Commun. **120**, 337 (2001).
[11] S. Matsumoto, E. Q. Xie, and F. Izumi, Diamond Related Materials **8**, 1175 (1999).
[12] E. Horvath-Bordon *et al.*, Angew. Chem. Int. Ed. **46**, 1476 (2007).
[13] J. Sjoberg, G. Helgesson, and I. Idrestedt, Acta Crystallogr., Sect. C: Cryst. Struct. Commun. **47**, 2438 (1991).
[14] X. Li and R. Jeanloz, Phys. Rev. B **36**, 474 (1987).
[15] H. K. Mao, J. Xu, and P. M. Bell, J. Geophys. Res. **91**, 4673 (1986).
[16] G. N. Greaves, C. R. A. Catlow, G. E. Derbyshire, M. I. McMahon, R. J. Nelmes, and G. van der Laan, Nature Mater. **7**, 827 (2008).
[17] A. P. Hammersley, S. O. Svensson, M. Hanfland, A. N. Fitch, and D. Hausermann, High Press. Res. **14**, 235 (1996).
[18] J. Rodriguez-Carvajal, Physica B **55**, 192 (1993).
[19] R. Dovesi *et al.*, *CRYSTAL 2006 User's Manual* (University of Torino, Torino, Italy, 2006).
[20] A. Becke, J. Chem. Phys. **98**, 5648 (1993).
[21] K. Burke, M. Enzerhof, and J. Perdew, Chem. Phys. Lett. **265**, 115 (1997).
[22] J. Binkley, J. Pople, and W. Hehre, J. Am. Chem. Soc. **102**, 939 (1980).
[23] W. Kraus and G. Nolze, J. Appl. Crystallogr. **29**, 301 (1996).
[24] F. Birch, Phys. Rev. **71**, 809 (1947).
[25] J. S. Loveday, R. J. Nelmes, W. G. Marshall, J. M. Besson, S. Klotz, and G. Hamel, Phys. Rev. Lett. **76**, 74 (1996).
[26] F. Datchi, S. Ninet, M. Gauthier, A. M. Saitta, B. Canny, and F. Decremps, Phys. Rev. B **73**, 174111 (2006).
[27] J. Liu, T. Sekine, and T. Kobayashi, Solid State Commun. **137**, 21 (2006).